

Birefringence-induced mode-dependent tuning of liquid crystal infiltrated InGaAsP photonic crystal nanocavities

M. A. Dündar, H. H. J. E. Kicken, A. Yu. Silov, R. Nötzel, F. Karouta, H. W. M. Salemink, and R. W. van der Heijden

Citation: [Applied Physics Letters](#) **95**, 181111 (2009); doi: 10.1063/1.3259814

View online: <http://dx.doi.org/10.1063/1.3259814>

View Table of Contents: <http://scitation.aip.org/content/aip/journal/apl/95/18?ver=pdfcov>

Published by the [AIP Publishing](#)

Articles you may be interested in

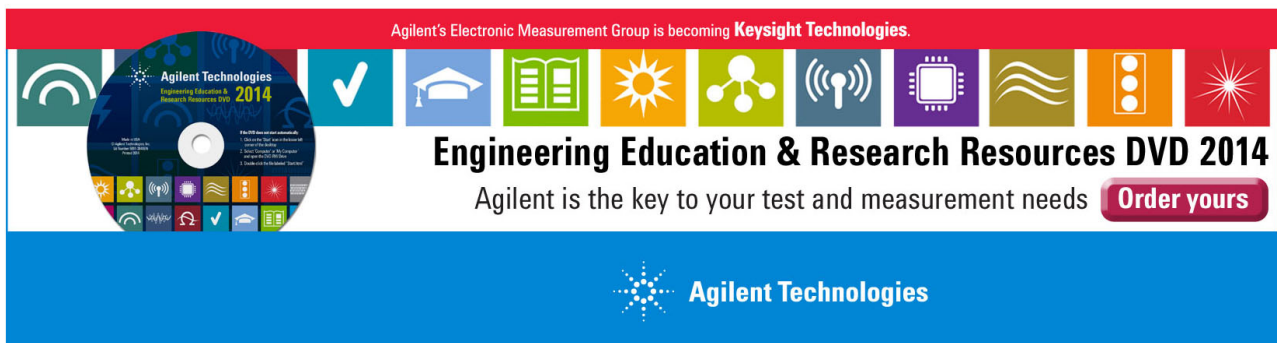
[Tunable and rotatable polarization controller using photonic crystal fiber filled with liquid crystal](#)
Appl. Phys. Lett. **96**, 241104 (2010); 10.1063/1.3455105

[Optical tuning of three-dimensional photonic crystals fabricated by femtosecond direct writing](#)
Appl. Phys. Lett. **87**, 091117 (2005); 10.1063/1.2037862

[Tuning photonic crystal nanocavity modes by wet chemical digital etching](#)
Appl. Phys. Lett. **87**, 021108 (2005); 10.1063/1.1992656

[Fabrication of high-quality-factor photonic crystal microcavities in InAsP/InGaAsP membranes](#)
J. Vac. Sci. Technol. B **22**, 875 (2004); 10.1116/1.1701848

[Polarization switching and induced birefringence in InGaAsP multiple quantum wells at 1.5 \$\mu\$ m](#)
J. Appl. Phys. **91**, 4090 (2002); 10.1063/1.1429794

The advertisement features a red header with the text 'Agilent's Electronic Measurement Group is becoming Keysight Technologies.' Below this is a row of ten colorful icons representing various engineering and research fields: a Wi-Fi symbol, a checkmark, a graduation cap, an open book, a sun, a network diagram, a radio tower, a microchip, a sine wave, a vertical bar chart, and a starburst. To the left of these icons is a DVD-ROM with the text 'Agilent Technologies Engineering Education & Research Resources DVD 2014'. Below the icons, the text reads 'Engineering Education & Research Resources DVD 2014' and 'Agilent is the key to your test and measurement needs'. A red button with white text says 'Order yours'. At the bottom, the Agilent Technologies logo and name are displayed on a blue background.

Birefringence-induced mode-dependent tuning of liquid crystal infiltrated InGaAsP photonic crystal nanocavities

M. A. Dündar,^{1,a)} H. H. J. E. Kicken,¹ A. Yu. Silov,¹ R. Nötzel,¹ F. Karouta,¹
H. W. M. Salemink,² and R. W. van der Heijden¹

¹COBRA Research Institute, Eindhoven University of Technology, P.O. Box 513, NL-5600 MB Eindhoven, The Netherlands

²Kavli Institute of NanoScience, Delft University of Technology, P.O. Box 5053, NL-2600 GB Delft, The Netherlands

(Received 17 July 2009; accepted 16 October 2009; published online 6 November 2009)

Mode-dependent shifts of resonant frequencies of cavities in liquid crystal (LC) infiltrated planar photonic crystals (PhC) are experimentally observed when the temperature is varied across the LC ordering transition. The shifts can be in opposite directions, even for two very similar nearly degenerate modes. The behavior is attributed to the different interactions of the modes with the two components of the refractive index of the LC infill and directly demonstrates that at least a substantial amount of the LC is oriented perpendicular to the PhC-hole axis. © 2009 American Institute of Physics. [doi:10.1063/1.3259814]

Photonic crystal nanocavities confine light into small modal volumes (V) with high quality factors (Q). A high Q/V ratio and the ability to tune the resonant frequencies make nanocavities attractive both for fundamental research and for applications. So far, they have been used for realizations of ultralow threshold lasers,¹ optical switches,² and add-drop filters.³ Most applications require fast, large, and active tuning of the resonant frequencies. Therefore, tuning mechanisms have been demonstrated that rely on changing the effective refractive index via temperature⁴ or by inserting scanning probe tips⁵ inside the air holes. Another promising approach is to change the refractive index of the cavity environment by infiltrating liquids. Liquid crystals (LC) have attracted much attention due to the ability to change the effective refractive index of the cavity by temperature or electric field. Infiltration techniques and the effects of the infiltrated LC have been widely studied, in particular for two-dimensional photonic crystal structures.^{6–10} In these studies, shifts of the bandgap edges and the lasing mode have been observed by adjusting either temperature or electric field. None of these studies has demonstrated the birefringent effect of the LC on the cavity resonances.

In this letter, we present evidence for the birefringent effect of the infiltrated LC from the temperature tuning of InGaAsP nanocavity modes. We show frequency shifts in opposite directions with varying temperature of two nearly degenerate modes, which is attributed to the opposite temperature dependence of the ordinary and the extraordinary refractive index of the LC. The presence of the birefringent effect is due to the electric field configuration of the resonant modes with respect to the distribution of an in-plane component of the LC orientation.

A hexagonal photonic crystal with cavities was made in a 220 nm thick InGaAsP membrane which contains a single layer of self-assembled InAs quantum dots¹¹ (density $3 \times 10^{10} \text{ cm}^{-2}/\text{layer}$). The pattern was defined in a 350 nm thick ZEP 520 resist by 30 keV electron beam lithography and subsequently transferred to an underlying 400 nm

thick SiNx mask layer. Next, the pattern was etched in an InP-InGaAsP-InP layer stack, by inductively coupled plasma etching using $\text{Cl}_2:\text{Ar}:\text{H}_2$ chemistry. The final step consisted of selective wet chemical etching of InP to leave a free standing InGaAsP membrane using a $\text{HCl}:\text{H}_2\text{O}=4:1$ solution at 2°C . The six air holes around a single missing air hole cavity were modified by changing their size and/or positions in order to achieve high- Q .¹² Figure 1(a) shows the scanning electron microscope (SEM) image of a fabricated InGaAsP nanocavity having a lattice spacing (a) of 480 nm and radius-to-lattice spacing ratio (r/a) of 0.3. The radius of the six modified holes is reduced by 33 nm and the center positions are shifted radially outwards by 13 nm.

The LC 4-pentyl-4' cyanobiphenyl (5CB, Merck), which has the nematic-isotropic phase transition temperature, or clearing temperature, T_c at 35°C , is infiltrated under ambient pressure. This is carried out by putting a drop of LC on the sample, while the sample and the LC are heated above T_c . The excess liquid is blown off the sample by dry nitrogen. The remaining LC thickness on the top of the sample is unknown. Since the hole infiltration is driven by capillary pressure effects, good wetting of the LC to the surface is essential. Contact angles were inspected occasionally, and are typically below 15° . From the shift of the cavity resonances after infiltration, it can be concluded that the holes are, at least substantially, filled, which is the ultimate proof for good and sufficient wetting. Ideally, all of the environment of the membrane should consist of LC as schematically sketched in Fig. 1(b). To investigate the temperature tuning, the infiltrated sample is placed on a heating stage. A photo-

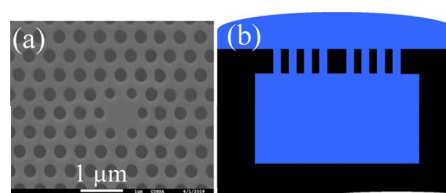


FIG. 1. (Color online) (a) SEM image of the modified InGaAsP nanocavity. (b) Schematic of ideal configuration of infiltrated LC into a PhC nanocavity.

^{a)}Electronic mail: m.dundar@tue.nl.

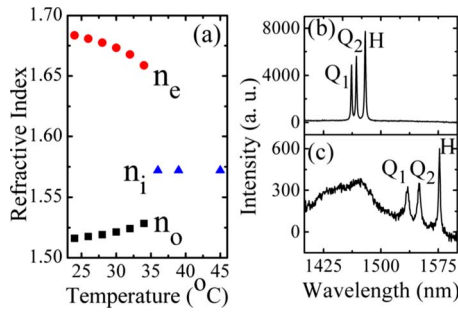


FIG. 2. (Color online) (a) Temperature dependence refractive index change of the LC. (b) PL spectrum of the nanocavity before the infiltration. (c) After the infiltration of the LC.

luminescence (PL) experiment is conducted by using a continuous wave He-Ne laser ($\lambda=632$ nm). An NA=0.5 100 \times optical microscope objective is used for both excitation of the cavities and collection of the PL. The relative strengths of the modes depend on the emission lobes of the cavities and, therefore, they are influenced by the relatively low NA of the objective, so the mode strengths should not be compared. After dispersing the PL in a 35 cm focal length monochromator, the collected signal is detected by a liquid nitrogen cooled InGaAs camera.

Figure 2(a) represents the temperature dependence of the ordinary (n_o) and the extraordinary (n_e) refractive index of the LC 5CB for the wavelength of 1.5 μ m, calculated from the parameters given in Ref. 13. The n_o and the n_e have an opposite temperature dependence, which varies slightly with temperature below T_c and shows an abrupt change at $T_c=35$ $^{\circ}$ C, when both n_e and n_o become equal to the isotropic refractive index n_i . Figure 2(b) shows the PL spectrum collected from the nanocavity as shown in Fig. 1, before infiltration. The modes are identified by a systematic investigation of photonic crystals (PhC)-cavities for varying lattice spacings and by comparison with known spectra of this type of cavities.¹⁴ The peaks occurring at 1461 and 1468 nm are quadrupole modes, referred to as the Q_1 -mode and the Q_2 -mode, respectively, having Q values up to 1000. The Q_1 -mode and the Q_2 -mode are degenerate in ideal cavities but in practice are split due to fabrication tolerances. The peak occurring at 1479 nm is the hexapole mode, referred as the H-mode, with a Q value 900. Figure 2(c) shows the spectrum of the same cavity after the infiltration of the LC, which is done with the LC in the nematic state. All resonant modes are redshifted by more than 70 nm. The redshift is somewhat smaller than expected from simulations (~ 100 nm), so that the complete filling of Fig. 1(b) is not realized. Presumably, the space below the membrane is not filled. This may result in increased scattering but the Q is still high enough to clearly resolve the resonances. Figure 2(b) shows that the Q_1 -mode and the Q_2 -mode are split by 7 nm before the infiltration. Figure 2(c) shows that the splitting is increased to 15 nm after the infiltration. The increase in the splitting shows that the two modes respond differently to the infill of the holes, which could be the result of different overlaps of the modes with the holes. The intensities and the Q values of the resonant modes are significantly decreased after the infiltration due to the lower refractive index contrast between the semiconductor membrane and the surrounding medium.

To investigate the possible influence of the LC orientation on the nanocavity modes, the temperature is increased

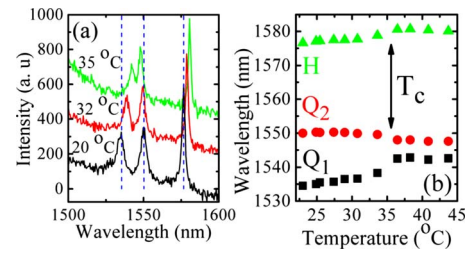


FIG. 3. (Color online) (a) PL emission of the LC infiltrated nanocavity at three different temperatures, 22 $^{\circ}$ C, 32 $^{\circ}$ C, and 35 $^{\circ}$ C. (b) The resonant wavelength shift of the modes with the increase of the temperature from 22 $^{\circ}$ C to 44 $^{\circ}$ C.

from 22 $^{\circ}$ C to 44 $^{\circ}$ C across the clearing temperature of $T_c=35$ $^{\circ}$ C. Figure 3(a) represents three PL spectra collected from the LC filled cavity at three different temperatures, one (22 $^{\circ}$ C) is well below and two (32 $^{\circ}$ C and 35 $^{\circ}$ C) are near T_c . Figure 3(b) shows the temperature dependent wavelength shift of the three modes. As the temperature increases from 22 $^{\circ}$ C to 34 $^{\circ}$ C, the Q_1 -mode and the H-mode, redshift by more than 3 and 2 nm, respectively. The redshift can be partly accounted for by the temperature dependence of the refractive index of the semiconductor, corresponding approximately to 0.1 nm/K.¹⁵ However, the Q_2 -mode exhibits a small blueshift around 0.5 nm. Near T_c , the Q_1 -mode and the H-mode show an abrupt redshift by more than 4 and 2 nm, respectively, while the Q_2 -mode is abruptly blueshifted by more than 1.5 nm. Above the transition temperature, there is no significant shift in the modes observed because the refractive index of the LC does not change in the isotropic state.

Our experimental results can be explained if the Q_2 -mode is dominated by the n_e , while the Q_1 -mode and H-mode are dominated by the n_o . The electric field of the cavity mode is in the plane of the PhC (TE-polarization), perpendicular to the hole axis. This requires that at least a substantial fraction of the LC is aligned in the plane, i.e., perpendicular to the hole axis. Since different modes, including degenerate ones, have different E-field profiles, the relative contributions of n_e and n_o to the effective refractive index in the holes may vary between modes. Even though the change in the refractive index is larger for the n_e than for the n_o , the data show that the observed blueshift for the Q_2 -mode is smaller than the obtained redshift for the Q_1 -mode and the H-mode. The reason is that even if the LC orientation is completely in-plane, there is still a distribution of orientations between the E-field and the LC orientation.

The LC orientation is determined by sidewall anchoring, surface energy, and molecular elasticity. Depending on these effects, three LC molecular orientations inside small diameter voids are theoretically proposed as follows: uniform axial, planar polar, and escaped radial, as sketched in Fig. 4.¹⁶ For the uniform axial orientation, Fig. 4(a), only n_o would be relevant for the TE-polarized cavity modes. Indeed, several letters suggest this orientation inside photonic crystal holes, notably in large hole diameter Si,⁸ and in deeply etched (InGa)(AsP).¹⁷ In other letters, evidence is presented for the escaped radial configuration [Fig. 4(b)], particularly well below T_c ,^{9,18} which has a significant amount of in-plane orientation. Only in one occasion so far,¹⁸ a very small blueshift, occurring well below T_c , has been reported and attributed to the n_e -contribution, but at the transition there was still a redshift.

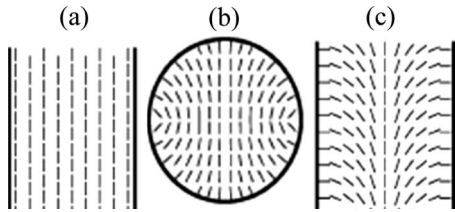


FIG. 4. Schematic of (a) axial uniform, (b) planar, and (c) escaped radial type of the LC alignment in the holes.

In order to investigate the persistence of the effect, the resonant frequency shifts at T_c were investigated for different nanocavities; all fabricated on the same chip and thus subjected to the same processing conditions. The cavities are of the type shown in Fig. 1, and only differ by slight variations of the surrounding hole geometry. Two examples of nanocavities, with the same a and r/a as the cavity in Fig. 1 are given in Figs. 5(a) and 5(b). In one cavity, the radii of the six surrounding holes are reduced by 33 nm and their center positions are displaced by 24 nm. For the other cavity, the radii are reduced by 20 nm, while the center positions are left unchanged. We refer to these cavities as Cc24_r33 and Cc0_r20, respectively. Both cavities accommodate the same Q_1 , Q_2 , and H-modes as the cavity in Fig. 3. Figure 5(a) shows that all three modes of the cavity Cc24_r33 are redshifted by more than 2, 8, and 5 nm, respectively, including an abrupt increase at the clearing temperature. Below the clearing temperature, the Q_1 -mode and the Q_2 -mode accidentally appear at the same wavelength. At the clearing temperature, the near-degeneracy of the modes is lifted and they suddenly split by more than 5 nm. This might be caused by the orientational effects of the LC but also by unequal filling of the holes. Figure 5(b) shows results from the cavity Cc0_r20. Here only the Q_1 -mode redshifts by more than 6 nm at T_c . The Q_2 -mode and the H-mode are blueshifted by more than 9 and 1.5 nm, respectively. All three modes show abrupt changes at the clearing temperature. The different behavior of the very similar cavities Cc24_r33 and Cc0_r20 show that the orientation of the LC inside the voids is not due to an intrinsic molecule-wall interaction, but may be randomly determined by varying surface properties of the etched holes. A variable LC orientation in the holes, depending on variations of the etched surface conditions, was also concluded on different grounds in previous letter.⁹ Since the orientation of the LC molecules inside the PhC holes is apparently varying, no model calculations have been undertaken to fit the frequency shifts. In addition, it should be

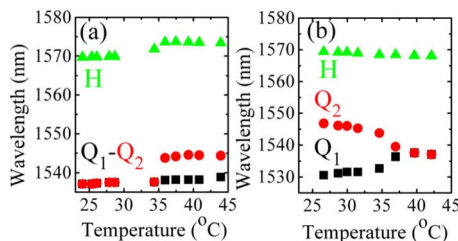


FIG. 5. (Color online) Temperature dependence resonant wavelengths change of (a) the cavity Cc24_r33 and (b) the cavity Cc0_r20.

noted that the optical properties of nonuniformly polarized LCs in small geometries may be exceedingly complex.¹⁹

In this letter, we have demonstrated the mode-dependent tuning of LC infiltrated InGaAsP nanocavity modes, which is attributed to the birefringent properties of the LC. The modes exhibit either a blueshift or a redshift at the LC clearing temperature, depending on the LC orientation. The results are consistent with both the planar and the more likely escaped radial type of the LC configuration inside the PhC holes. A possible enhancement of the effects due to unequal filling of the holes cannot be ruled out but unequal filling cannot explain the opposite tuning behavior. The effects are dominated by varying surface conditions and are potentially interesting for device applications.

The authors gratefully acknowledge useful discussions with C.W.M. Bastiaansen, D.J. Broer, and A. Fiore and thank P. A. M. Nouwens, B. Smalbrugge, E. J. Geluk, P. J. van Veldhoven, and T. de Vries for their help in the fabrication processes. Part of this research is supported by NanoNed, a technology program of the Dutch Ministry of Economic Affairs via the foundation STW. This work is part of the research program of the “Stichting voor Fundamenteel Onderzoek der Materie (FOM),” which is financially supported by the “Nederlandse Organisatie voor Wetenschappelijk Onderzoek (NWO).”

¹O. Painter, R. K. Lee, A. Scherer, A. Yariv, J. D. O’Brien, P. D. Dapkus, and I. Kim, *Science* **284**, 1819 (1999).

²H. Takeda and K. Yoshino, *Phys. Rev. B* **67**, 073106 (2003).

³H. Takano, Y. Akahane, T. Asano, and S. Noda, *Appl. Phys. Lett.* **84**, 2226 (2004).

⁴A. Faraon, D. Englund, I. Fushman, J. Vučković, N. Stoltz, and P. Petroff, *Appl. Phys. Lett.* **90**, 213110 (2007).

⁵A. F. Koenderink, M. Kafesaki, B. C. Buchler, and V. Sandoghdar, *Phys. Rev. Lett.* **95**, 153904 (2005).

⁶S. W. Leonard, J. P. Mondia, H. M. Van Driel, O. Toader, S. John, K. Busch, A. Birner, and U. Goesele, *Phys. Rev. B* **61**, R2389 (2000).

⁷Ch. Schuller, F. Klopff, J. P. Reithmaier, M. Kamp, and A. Forchel, *Appl. Phys. Lett.* **82**, 2767 (2003).

⁸G. Mertens, T. Roder, H. Matthias, H. Marsmann, H. S. R. Kitzerow, S. L. Schweizer, C. Jamois, R. B. Wehrspohn, and M. Neubert, *Appl. Phys. Lett.* **83**, 3036 (2003).

⁹R. Ferrini, J. Martz, L. Zuppiroli, B. Wild, V. Zabelin, L. A. Dunbar, R. Houdré, M. Mulot, and S. Anand, *Opt. Lett.* **31**, 1238 (2006).

¹⁰B. Maune, M. Loncar, J. Witzens, M. Hochberg, T. Baehr-Jones, D. Psaltis, A. Scherer, and Y. Qiu, *Appl. Phys. Lett.* **85**, 360 (2004).

¹¹R. Nötzel, S. Anantathanasarn, R. P. J. van Veldhoven, F. W. M. van Otten, T. J. Eijkemans, A. Trampert, B. Satpati, Y. Barbarin, E. A. J. M. Bente, Y. S. Oei, T. de Vries, E. J. Geluk, B. Smalbrugge, M. K. Smit, and J. H. Wolter, *Jpn. J. Appl. Phys., Part 1* **45**, 6544 (2006).

¹²H.-G. Park, J.-K. Hwang, J. Huh, H.-Y. Ryu, S.-H. Kim, J.-S. Kim, and Y.-H. Lee, *IEEE J. Quantum Electron.* **38**, 1353 (2002).

¹³J. Li and S. T. Wu, *J. Appl. Phys.* **95**, 896 (2004).

¹⁴M. Shirane, S. Kono, J. Ushida, S. Ohkouchi, N. Ikeda, Y. Sugimoto, and A. Tomita, *J. Appl. Phys.* **101**, 073107 (2007).

¹⁵B. Wild, R. Ferrini, R. Houdré, M. Mulot, S. Anand, and C. J. M. Smith, *Appl. Phys. Lett.* **84**, 846 (2004).

¹⁶S. V. Burylov, *Sov. Phys. JETP* **85**, 873 (1997).

¹⁷P. El-Kalassi, R. Ferrini, L. Zuppiroli, N. Le Thomas, R. Houdré, A. Berrier, S. Anand, and A. Talneau, *J. Opt. Soc. Am. B* **24**, 2165 (2007).

¹⁸Ch. Schuller, J. P. Reithmaier, J. Zimmermann, M. Kamp, A. Forchel, and S. Anand, *Appl. Phys. Lett.* **87**, 121105 (2005).

¹⁹E. Brasselet, N. Murazawa, H. Misawa, and S. Juodkazis, *Phys. Rev. Lett.* **103**, 103903 (2009).